OUTLET WORKS OF SPILLWAY TUNNELS

BY
J. M. K. DAKE *
AND
J. R. D. FRANCIS **

Introduction

1. A problem which frequently occurs in hydraulic engineering practice is to spread and dissipate the energy of a concentrated, fast-flowing stream of water, so that it does not cause erosion of the valley into which it flows. Many forms of stilling basin have been designed (See references [1] and [2]) and have been tested for satisfactory operation, but these have been mainly for spillways where the incoming stream has a free surface. There is less information about the case of a pipe or tunnel flowing full-bore and discharging upon a plane surface at the level of the pipe invert. This case may arise at the outlet of tunnels from bell-mouth spillways at irrigation outlets and at the outlet of diversion tunnels.

2. Water speeds of 80 feet per second or more have been recorded and considerable damage to valley bed or to the dam itself could result, unless adequate energy dissipation were achieved. For an efficient stilling basin it is desirable to spread the stream as quickly as possible, thereby making the influence of bed stress felt over a wider area and into a higher proportion of the depth of the stream. The spreading of such a high speed jet is, of course, quite different hydraulically from the problem of spreading the far lower speeds of an irrigation supply into porous soils [3].

3. Besides encouraging a more efficient energy dissipation by friction in the stilling basin, an adequate spreading and so shallowing of a fast flow encourages the formation of a hydraulic jump which dissipates still more energy. The smaller the upstream depth at a jump for a given discharge, the more energy will be dissipated. Since in general the depth of flow in the channel downstream of the basin is fixed, the importance of a well expanded flow in the basin can be understood. However, if this expansion is too rapid, separation of the flow from the walls can occur. The separation surface acts as a solid boundary, restricting the flow, making it behave as would occur in a channel constriction. On the other hand, a too gradual expansion brings about a waste of structural material and excessive excavation. A poorly designed geometrical shape of the expansion may also

* M. Sc. Tech. On leave from Kwame Nkrumah University of Science and Technology, Kumasi, Ghana.
** Manchester College of Science and Technology.

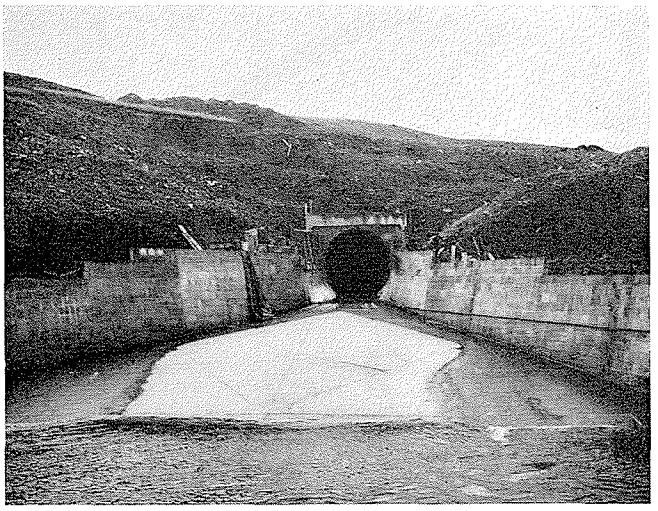

1/ The outlet of the spillway tunnel at the Balderhead dam of the Tees Valley Water Board (Consulting Engineers : Sandeman, Kennard & Partners). The tunnel is 14 ft diameter. The pyramidal hump in the foreground was designed with the aid of model tests.

La sortie de la galerie d'évacuation des crues au barrage de Balderhead (Maître de l'œuvre : Tees Valley Water Board. Ingénieurs-Conseils : Sandeman, Kennard & Partners). Le diamètre de la galerie est égal à 4,25 m. La bosse en forme de pyramide à l'avant-plan a été étudiée à l'aide d'essais sur modèle réduit.

produce excessive wave heights which might well overtop the side walls.

4. One method of encouraging a jet to spread is to impose upon it a pressure gradient transverse to the initial direction of motion. In an open channel flow this is tantamount to sloping the bed across the flow, and for symmetry implies that a cross section of the bed has a triangular shape with a crest at the centreline. On an initially flat surface, such a device demands that the bed shall rise temporarily to afford the elevation from which the pressure gradient develops. The rise is not carried on indefinitely, so that the result is a pyramidal « hump », first rising, then falling in the direction of motion, with a triangular cross section across the flow.

5. The adequate spreading of a fast flow also enables the basin to be laid shallower or made shorter. This is because in many cases, the depth of flow in the downstream channel of a spillway outlet work is smaller than that required to form a hydraulic jump, so that the basin is laid deeper to provide the necessary depth. A shallower incoming stream would provide a higher conjugate-depth ratio at the jump and thereby reduce the necessity for a deep basin.

Alternatively the shallow upstream depth for a given down-stream depth produces a hydraulic jump in a position further upstream and, therefore, makes it possible for a shorter basin to be used.

6. Though the properties of hydraulic jumps in channels of rectangular cross section and of uniform width are well-known and can easily be calculated, it is otherwise with jumps in expanding channels. Kuznetzow [4] has devised an empirical formula to fit observations which Unny [5] has improved. Nevertheless, it is fair to state that most engineers faced with an important design of a stilling basin would prefer to use an *ad hoc* hydraulic model, particularly if the incoming jet was not of rectangular section, and its spreading from a circular pipe had first to be achieved. It was the purpose of the experiments to investigate the spreading of such jets and the resultant hydraulic jumps.

Experimental work

7. The experiments, carried out in the Civil Engineering Laboratories of the Manchester College of Science and Technology, were to a small size, but are not to be regarded as a model of any specific scheme. Thus no scale ratio can be quoted. The size was however thought to be large enough to ensure that there were no surface tension effects present; the Froude scaling law may be used with fair confidence to extrapolate the results to a larger size.

8. The general arrangement of the apparatus is shown in Figure 1. A jet of water issued from a 6 inch delivery pipe and spread on a smooth, varnished, flat plywood board set up on top of an 8 ft long × 4 ft wide × 3 ft deep cistern. The horizontal plane of the 6 ½ ft × 3 ft board contained the line of the invert of the delivery pipe. The depth of flow over every point on the board was measured using a micrometer gauge capable of reading accurately to 1/1,000th inch carrying a long pointed brass rod, and held firmly in a gauge carrier which could be moved on another carrier across the stream and which itself could slide up and down on rails supported and levelled on the sides of the cistern.

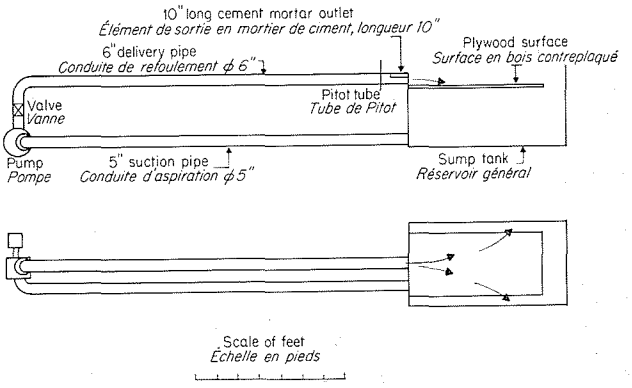

Diagram of experimental equipment. Upper figure is a side elevation, lower figure is a plan.

Schéma de l'installation expérimentale. En haut, vue de profil, en bas, vue en plan.

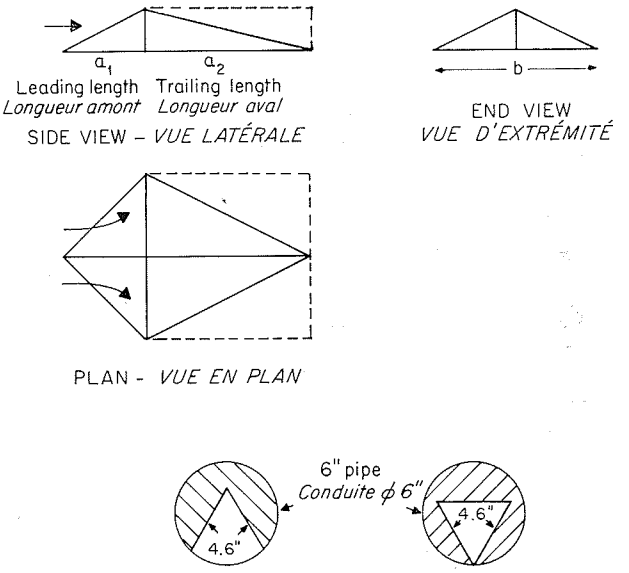

2/ Definition figures for (*a*) hump and (*b*) outlet geometry. Left lowest figure is the upright triangular outlet of equivalent diameter $d_e = 4$ in.; right lowest is inverted triangle $d_e = 3.2$ in. Dotted lines show outline of Class II humps.

Schémas de définition des caractéristiques géométriques de la bosse (a) et du profil aval (b). En bas, à gauche, la sortie triangulaire de diamètre équivalent $d_e = 10$ *cm; en bas, à droite, le triangle renversé avec* $d_e = 8$ *cm. Les lignes en pointillé indiquent la forme des bosses de classe II.*

9. In order, first, to be able to obtain higher speed jets and, second, to be able to test different outlet shapes, 10 inch long outlet fittings moulded from cement and sand mortar were fitted into the outlet end of the 6 inch delivery pipe for various tests.

10. The total energy head and direction of flow at particular points on the spreading floor were measured with a yaw-meter designed on the principle of the pitot-cylinder (sometimes called the « direction finding tube »). The pressures at two holes spaced 60° apart on a cylinder are balanced, when the direction of flow is along the bisector.

11. The pyramidal « humps » tested are defined by Figure 2 (*a*) and Table 1. Whilst Class I humps were designed primarily only to encourage quicker spreading of the outflowing jet of water, Class II humps were deliberately designed to split the flow into two. The dotted lines represent the bounding edges for Class II humps, the front view being the same for both classes.

TABLE 1 :

Dimensions of Humps

No.	Class I								Class II		
	1	2	3	4	5	6	7	8	9	10	11
a_1 (ins). . .	3	3	6	3	6	3	3	3	4	6	4
a_2 (ins). . .	6	6	6	6	3	6	6	6	4	4	4
b (ins). . . .	12	12	12	6	6	6	6	4	6	6	4
h (ins). . . .	2	1	2	2	1	1	1½	2	4	4	4

12. The preliminary investigations were aimed at the study of the characteristics of the undisturbed pattern of spreading without the introduction of pyramidal humps. Measurements included surface profiles for three different shapes of outlet: circular outlets (6 inch, 4 inch and 3.5 inch diameters—22 discharges in all); an upright triangular outlet (9 discharges); and an inverted triangular outlet (12 discharges) covering a range of outlet Froude Number $F_0 = U_0^2/gd_0$ up to 36.6 (see Fig. 2 (*b*). These measurements enabled comparison to be made between the three shapes of outlet to discover which gave the most rapid spreading. In these measurements a rectangular system of axes was used, x being along the tunnel axis, y vertically upward, and z transversely across the original flow direction.

13. In Figure 3 (*a* and *b*) are shown the total head H distribution across the stream at various sections and the corresponding directions of flow for two outflows. The total head curves fall sharply from approximately the same maximum value which extends to increasing z/d_0 as the sections of measurement are moved downstream. The maximum H/d_0 is 13.3 for $F_0 = 21.6$ and 9.1 for $F_0 = 15.5$. Thus, it may be concluded that there exists a core in the central region of the spreading jet for which the total head is constant and beyond which the total head decreases rapidly sideways. This must be due principally to the boundary layer which occupies an ever-increasing proportion of the depth as the flow becomes shall-

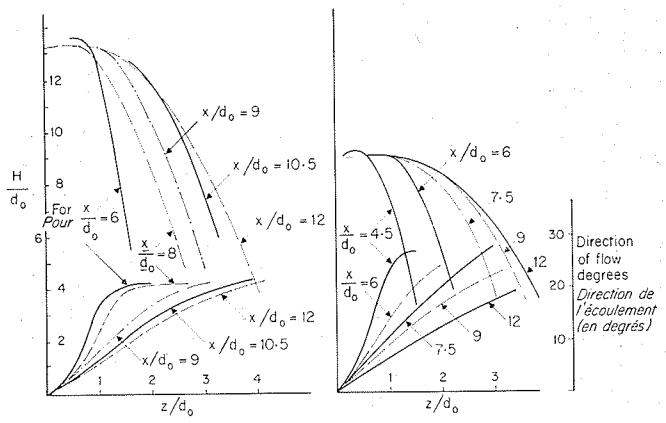

3/ Total head and flow direction curves in an unrestricted spreading jet. Left-hand graphs for $F_0 = 21.6$; right-hand for $F_0 = 15.5$. Upper graphs are for H/d_0; lower for direction θ.

Représentation graphique des charges totales et des directions d'écoulement dans un jet non limité et en cours d'étalement. Les graphiques à gauche correspondent à $F_0 = 21{,}6$, *ceux de droite à* $F_0 = 15{,}5$. *Les courbes supérieures correspondent à* H/d_0 *et les courbes inférieures à la direction* θ.

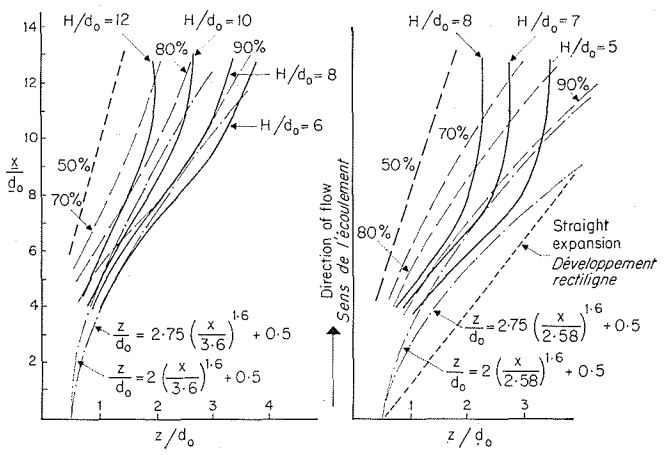

4/ Total head and flow distribution curves in an unrestricted spreading jet. Left-hand graphs for $F_o = 21.6$ ($E_o = 3.6$ ft) right-hand for $F_o = 15.5$ ($E_o = 2.5$ ft). Dashed lines show the percentage of the flow contained within them, and two suggested curves for channel expansions are shown. Full lines show total head contours.

Représentation graphique de la répartition des charges totales et de l'écoulement dans un jet non limité et en cours d'étalement. Les graphiques à gauche correspondent à $F_o = 21{,}6$ ($E_o = 1{,}10$ m), ceux de droite à $F_o = 15{,}5$ ($E_o = 0{,}76$ m). Les lignes en traits discontinus indiquent le pourcentage de l'écoulement qu'elles contiennent; la figure présente également deux courbes correspondant à des élargissements proposés pour le canal. Les lignes en traits pleins correspondent aux courbes de charge totale.

ower sideways. The same explanation may be given for the inward curvature of the total head contour lines in Figure 4. Since the flow under investigation is steady, the total head contours would approximate to the « streamlines ». The method of tracing the locus of an H/d_0 value from Figure 3 which was used in drawing the curves in Figure 4 did not take into account energy losses due to friction which become increasingly important farther downstream where the flow becomes shallower.

14. Figure 4 also indicates that the central core of maximum constant energy and axial velocity contains about 70 to 80 per cent of the entire flow even though it is only about a third of the width of the spreading jet. Thus in practice, side walls spaced wider than the streamlines containing this central core will make very little difference to the overall operation of a stilling basin as far as energy is concerned; and this is confirmed by tests on model stilling pools reported below.

15. The directional angle θ increases across each section from zero on the axis towards a maximum value corresponding to that which the bounding streamline (breadth of jet) makes with the x-direction. The farther downstream one moves the gentler the increase in the curvature.

16. From the streamlines which have been derived from the flow distributions of Figure 4 (*a* and *b*) useful approximations can be made for the vertical walls which would just confine a given proportion of the flow. Equations of the type :

$$\frac{z}{d_0} = C\left(\frac{x}{E_0}\right)^{1.6} + 0.5$$

are shown on Figure 4, and it will be seen that for $C = 2$ about 85 % of the flow is contained, and for $C = 2.75$ about 95 % of the flow is contained. In these equations :

- z is the horizontal distance perpendicular to the x-axis;
- d_0 is the outlet diameter;
- x is the longitudinal distance from the outlet;

and E_0 is the design outlet velocity head ($U_0^2/2g$).

The expansions, which are similar to those suggested by Rouse, Bhoota and En-Yun Hsu [6] for expansions from a rectangular open channel into another rectangular open channel, were tested for stilling pools as reported below.

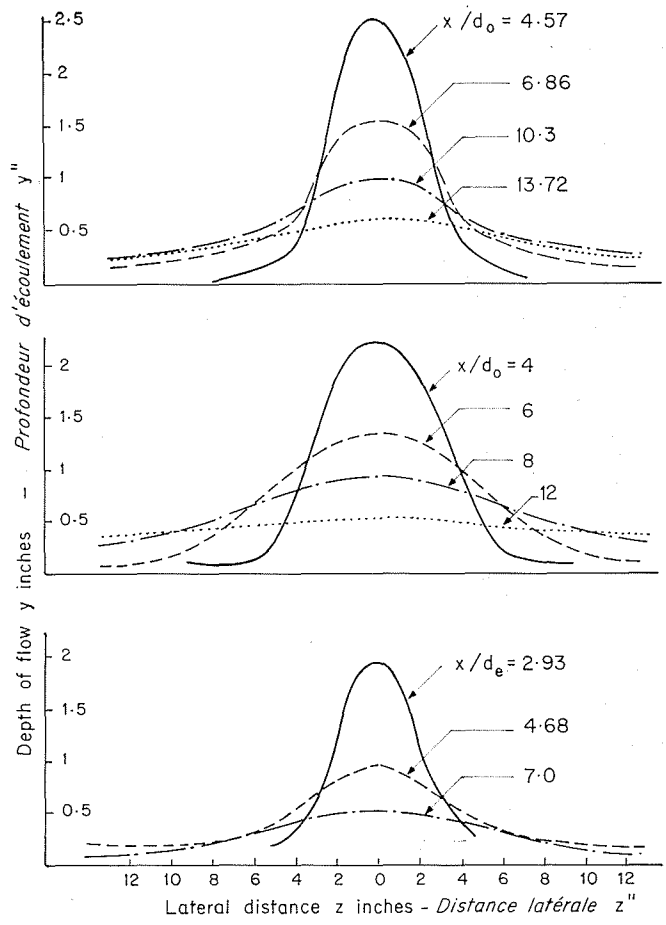

5/ Surface profiles across the jet axis of an unrestricted spreading jet. Top group of curves are for the circular outlet; middle group for upright triangular outlet; bottom group for inverted triangular outlet.

Profils superficiels à travers l'axe d'un jet non limité et en cours d'étalement. Le graphique supérieur correspond à l'orifice de sortie circulaire; celui du milieu, à l'orifice triangulaire debout; celui du bas, à l'orifice triangulaire inversé.

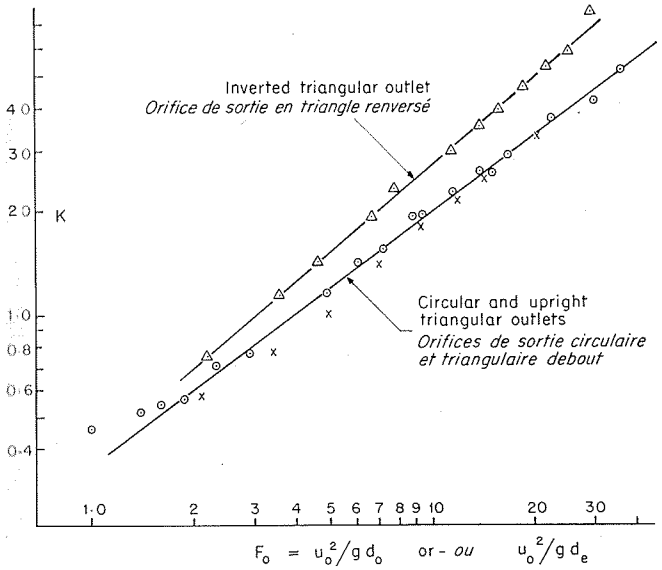

6/ Variation of function K with the outlet Froude number (K is the slope of the y_m/d_o against d_o/x graph in any one test). Upper line for inverted triangular outlet; lower line for circular and upright triangular outlets.

Variation de K en fonction du nombre de Froude à la sortie (K étant la pente de la courbe y_m/d_o *en fonction de* d_o/x *correspondant à un seul essai quelconque). La courbe supérieure correspond à l'orifice de sortie en triangle inversé, et celle du bas aux orifices de sortie circulaire et triangulaire debout.*

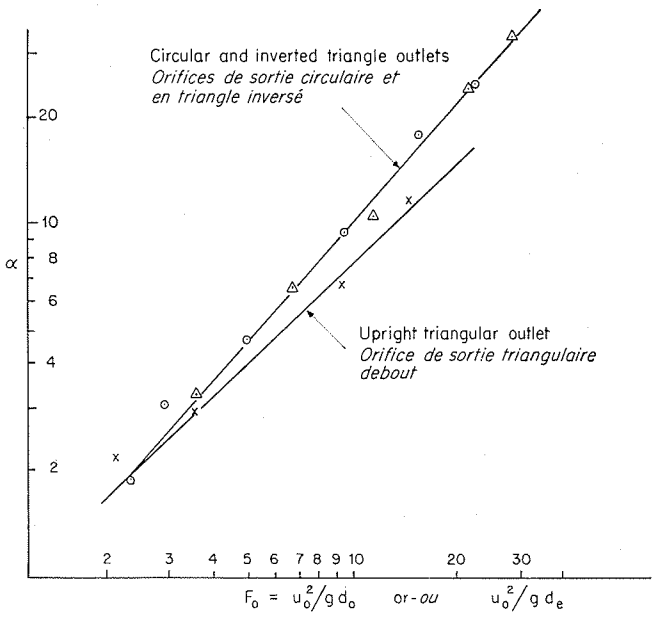

7/ Variation of the exponent index α with outlet Froude number. Upper line is for circular and inverted triangular outlet; lower for upright triangular outlet.

Variation de l'exposant α en fonction du nombre de Froude à la sortie. La courbe supérieure correspond aux orifices de sortie circulaire et triangulaire inversé, celle du bas, à l'orifice triangulaire debout.

17. Surface profiles across the flow are shown in Figure 5. Profiles both across and along the flow axis show striking resemblances to the velocity profiles of a symmetrical jet of incompressible fluid diffusing into an infinite space of the same fluid. Both phenomena are concerned with the conservation of momentum but the processes that give near-constant velocity and changing elevation to the water jet but varying velocity to the diffusing jet must clearly be somewhat different. The analogies will not be further prosecuted here and will be reported more fully in another place. It merely remains to remark that an empirical equation :

$$y = \frac{A_1 d_0^2 K}{x} \exp(-\alpha z^2/x^2)$$

is a useful approximation to the three-dimensional shape of the spreading water jet on a horizontal surface. The functions K and α were determined from the experiments, and both depend on the outlet Froude number $U_0^2/gd_0 = F_0$. The constant A_1 depends on the shape of the outlet. The functions are shown in figs. 6 and 7 and in the case of α represents average conditions below $z/d = 3$; above $z/d = 3$, the spreading is so gradual and the surface so unsteady with waves and ripples that the errors of measurement are too great to give a reliable estimate of α.

18. Comparisons have been made between the spreading of jets emerging from circular pipes and from those of triangular cross section, both with vertex in the uppermost and in the lowest positions. These show that the constant A_1 averages 0.80 to 0.85 for the circular and upright triangular outlets and between 0.6 and 0.7 for the inverted triangular outlet (i.e. with vertex at lowest point). The latter type of outlet therefore gives a *lower* water level at a given distance far from the outlet than the other two types, and so is rather better for spreading the jet.

Hump Tests.

19. A similar set of observations of water surface were made with eleven different sizes of hump in position on the horizontal surface. A typical comparison of water profiles with and without the hump is shown in Figure 8 (*a*). As was indeed expected, the tests showed that the effectiveness of a hump for spreading a jet of water from a tunnel depends on its width, height and leading length as well as on its position relative to the outlet and outflow speed. The tests have revealed that it is, in any case, desirable for the breadth of the hump to be at least one diameter of the outlet and the wider it is, the better. But the width must be reconciled with its height, since the effectiveness depends also on the side slope given by $2\,h/b$, see Figure 2. Too gentle a slope tends to reduce the hump into a thin plate, and thus reduces its effectiveness. A high hump, on the other hand, introduces a cavity behind the hump at relatively low efflux speeds. The leading length a_1 also shows marked effects. While it is desirable to make a_1 long, to delay cavity formation, it was observed during the tests

that too gentle a leading slope (h/a_1) would reduce the effectiveness of the hump.

20. The position of the hump (characterised by X, the distance from outlet to the crest of the hump) was observed to play an important part in its effectiveness in spreading the flow. If it is placed far downstream, a large cavity is formed behind it; while if it is too near the outlet, high speeds, i.e., high value of F_0, tend to rush over it, being hardly affected. Figure 8 (*b*) shows how the centreline water surface elevation y_m varies with x for two different values of F_0, with and without a hump at $X/d_0 = 1.75$. At low value of $1/x$ (i.e. large values of x) and at the low speed ($F_0 = 3$), the depth of flow is less with the hump than without it; the hump is therefore effectively spreading the flow. At the high speeds ($F_0 = 11$), the hump barely affects the depth of flow.

21. Much is said here about the formation of a cavity behind a hump because of certain effects it is likely to produce in a stilling basin. In the absence of any likelihood of oscillatory make-and-break activity due to the continual formation and collapse of the cavity arising from external forces being exerted on it, the cavity may not be objectionable. The experiments have revealed that the cavity itself encourages spreading. It provides slower streaming motion downstream after the water impinges on the bed and, in practice, it will be advisable to provide a pool behind the hump into which the water will fall. Cavity formation may be delayed by rounding the edges of the hump or by building its back into a well-rounded shape. This will inevitably reduce its effectiveness, especially at high flows which will tend to rush over the near-aerofoil form.

22. Taking into account the above points, hump No. 4 ($a_1 = 3$ in, $a_2 = 6$ in, $b = 6$ in, $h = 2$ in) was considered to be the best design among those tested in Class I in conjunction with a 4 inch diameter outlet. Hump No. 8 ($a_1 = 3$ in, $a_2 = 6$ in, $b = 4$ in, $h = 2$ in) was also considered satisfactory and was used for the model stilling basin tests described below. Table 2 gives suggested optimum positions for hump No. 4 for various ranges of outflow.

TABLE 2

Optimum Positions for Hump 4

HUMP POSITION X/d_o	APPROXIMATE RANGE OF OUTFLOW F_o
1.0	up to 7
1.25	7 to 10
1.5	9 to 15
1.75	12 to 19
2.0	19 to 25
2.25	25 to 30
2.5	30 to 40
3.0	above 40

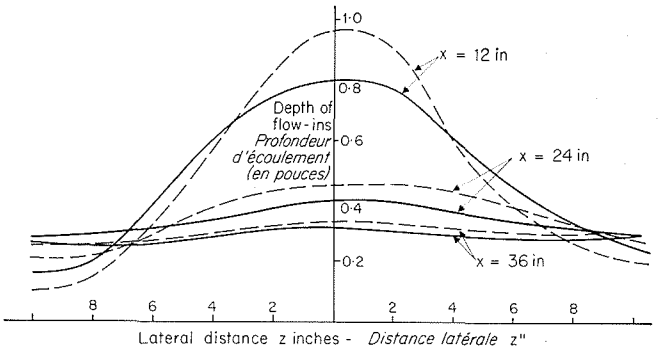

8 a/ Surface profiles across jet axis with and without a hump. Circular outlet pipe running at $F_o = 4.0$. Dotted lines are profiles without a hump; full lines with hump No. 6 at $X = 6$ in.

Profils superficiels à travers l'axe du jet, avec et sans bosse. La conduite circulaire de sortie fonctionne avec $F_o = 4{,}0$. Les lignes en pointillé correspondent à des profils sans bosse, les lignes continues à des profils avec la bosse n° 6, implantée à $X = 15$ cm.

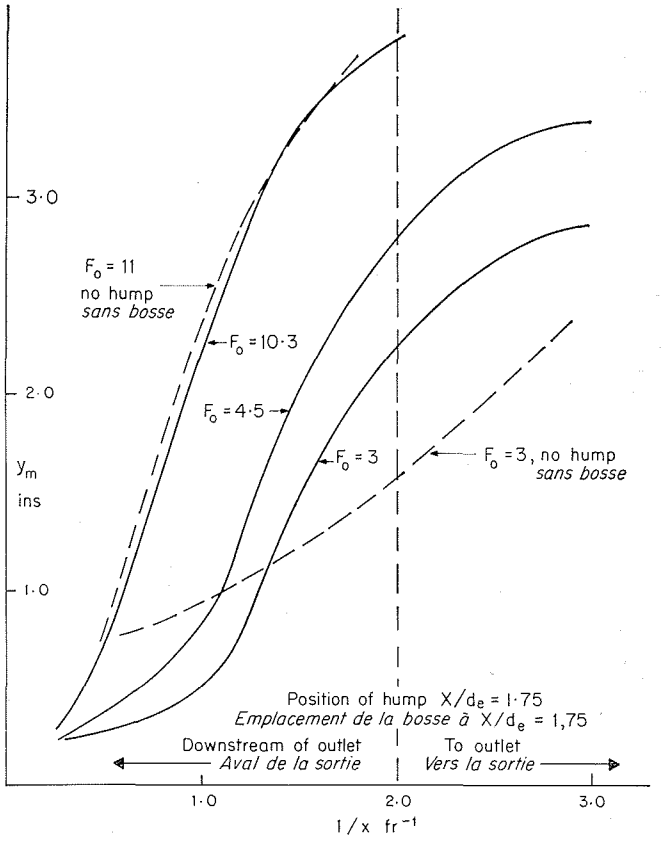

8 b/ Curves of depth on centreline y_m against reciprocal of distance from outlet $1/x$ showing effect of a hump. Dotted lines without a hump, full lines with hump at $X/d_o = 1.75$. Inverted triangular outlet.

Profondeurs à l'axe y_m en fonction de l'inverse de la distance de la sortie, 1/x, mettant en évidence l'influence de la présence d'une bosse. Les lignes pointillées correspondent au cas sans bosse, les lignes continues au cas d'une bosse en $X/d_o = 1{,}75$. Orifice de sortie en triangle inversé.

23. Even though the humps in Class II did not provide an absolute division of the flow, they provided almost an ideal spreading and would be recommended for use as such, especially for irrigation spreading works. They are unsuitable for stilling basins since they are unsatisfactory at high F_0 and, being large with considerable side gradients, would be expensive to build.

Tests on model stilling pools

24. Tests were performed on several models of complete stilling pools to obtain information on the effect of their geometry on their hydraulic performance. Each pool consisted of vertical walls diverging in plan on a horizontal floor, and had a sill or weir across its widest portion. The sill caused a hydraulic jump to occur upstream of it. The outlet pipe in all experiments was 4 in. diameter, but in each test the diverging walls were of a different plan shape. Where the walls had diverged to 32 in apart they were joined abruptly to parallel walls (see Fig. 9). Sills of different heights were tested at a number of distances from the pipe; and in the two cases (*a*) and (*b*) below the effect of a hump was also observed. The plan shape of the diverging walls were :

(*a*) Straight line;

(*b*) Curved to follow the streamlines containing 95 % of the flow of the unconfined jet;

(*c*) Curved to follow the 90 % streamlines;

(*d*) Curved to follow the 80 % streamlines.

In each case the curves were designed for an outlet kinetic head E_0 of 2.58 ft; i.e. an outlet Froude number $F_0 = 15.5$.

25. Each observation in each test consisted of a visual assessment of the outlet Froude number F_0 at which the fast flow in the basin began to override the end sill; at this stage the hydraulic jump had not fully formed. At lower values of F_0, the jump retired toward the outlet pipe and a length of slow, tranquil flow existed between the jump and where the water accelerated over the sill as a weir. The assessment of whether the jump was fully developed before the sill is of course a matter of personal opinion to some extent; but for a single observer the broad effects of variations of sill position and height, and curvature of walls should be seen consistently.

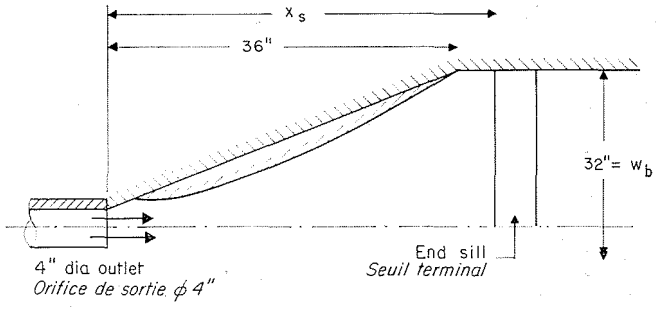

9/ Geometry of model stilling pool. Plan view showing straight expansion walls and one of the curved walls.
Caractéristiques géométriques du modèle du bassin de dissipation. Vue en plan d'une des parois rectilignes de raccordement au bassin et d'une des parois courbes.

One set of experiments carried out by one of us (JKMD) was for the condition when a great deal of jump turbulence still remained in the water at the sill; another set, kindly carried out for us by Mr J. Engmann, was for a more conservative condition with the jump nearer the outlet pipe and therefore more of the turbulent energy dissipated before the water reached the sill. Comparison of the results show that the maximum satisfactory E_0 for the first set is some 70 % to 100 % greater than that for the second set; thus the flows predicted as satisfactory by the two observers were in the ratio $\sqrt{1.7}$:1 to $\sqrt{2}$:1 i.e., 1.3:1 to, 1.4:1. The two observers' results probably represent the extremes between which the engineer must choose, using the lower discharges in cases where very tranquil flow is required (as when the sill is used as a measuring weir) and the higher discharges if great economy is required in the building of the stilling pool and if some high speeds can be tolerated in the downstream river.

26. Dimensional analysis can be used to give a relation between the outlet speed U_0, position of sill from outlet point x_s, the height of the sill h_s, and the ultimate width of the stilling basin w_b all for a given hydraulic performance. This relation is :

$$\text{Function of } \left(\frac{U_0^2}{g d_0}, \frac{h_s}{d_0}, \frac{x_s}{d_0}, \frac{w_b}{d_0}\right) = 0$$

or

$$\frac{h_s x_s}{d_0^2} = f\left(F_0, \frac{w_b}{d_0}\right)$$

The term $h_s x_s / d_0^2$ is broadly connected to the excavation required in a suitable pool; and its dependence on F_0, the outlet of Froude number, and w_b/d_0 is shown in Figures 10 and 11 from the experiments carried out.

27. Figure 10 shows the comparison for a straight-sided expansion when tested without a hump and when tested with hump No. 4. It shows that for a particular height of a broad-crested end sill at a particular distance away from the outlet for an ultimately wide basin (wider than the central core of energy concentration), the use of the hump increases by more than 15 % the Froude number at which the basin becomes ineffective, thus the flow (which is proportional to U_0) is increased by some 10 %. No remarkable differences in effectiveness are noticed for widths of $w_b/d_0 = 8$ and $w_b/d_0 = 6$, a result which confirms the deduction made above that once the width of the basin is sufficient as not to restrict the normal spreading behaviour of the jet or lie within the zone of maximum energy concentration, extra width of the basin adds no obvious advantages to its energy dissipation capabilities, provided that excessive shock wave fronts are not produced.

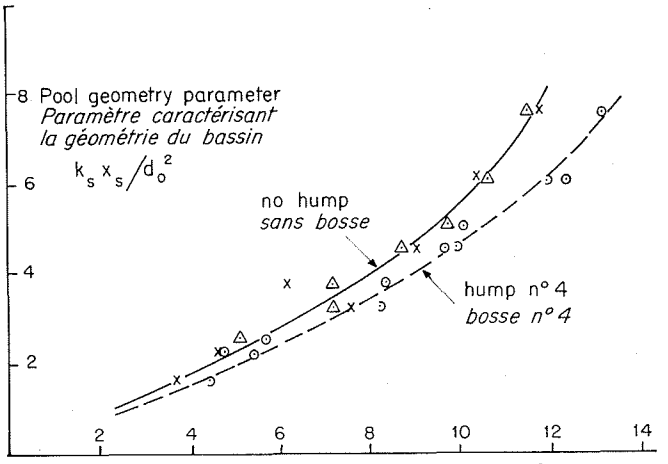

10/ Effect of sill proportions on satisfactory operation of a straight walled expansion pool. Upper graph without hump, lower with hump No. 4 at $X/d_o = 1.5$. Triangle points for $w/d_o = 8$; crosses $w/d_o = 6$ without a hump. Circles $w/d_o = 8$; half circles, $w/d_o = 6$ with hump No. 4.

Influence des dimensions du seuil sur le fonctionnement correct d'un bassin de dissipation à parois rectilignes. La courbe du haut correspond au cas sans bosse, celle du bas au cas avec la bosse n° 4 implantée en $X/d_o = 1{,}5$. Les points désignés par des triangles correspondent à $w/d_o = 8$, les croix à $w/d_o = 6$, sans bosse. Les cercles correspondent à $w/d_o = 8$ et les demi-cercles à $w/d_o = 6$ avec la bosse n° 4.

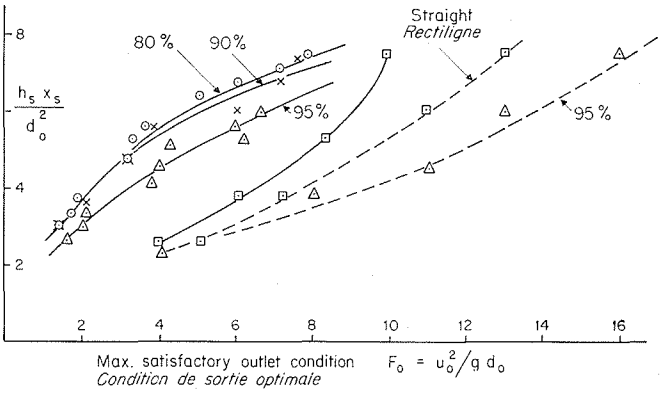

11/ Effect of sill height and distance on satisfactory operation of pools. Each pool has different side wall curve. Full lines are for experiments with conservatively low velocity, dotted lines for experiments with jump nearer the sill. Percentages refer to the walls which are curved to those percentage flow contours of a free-spreading jet.

Influence de la hauteur du seuil et de la distance sur le fonctionnement correct des bassins de dissipation. Chaque bassin présente une courbe de paroi latérale différente. Les lignes continues ont trait à des expériences réalisées avec des vitesses modestes, et les lignes pointillées à des expériences présentant un ressaut hydraulique situé plus près du seuil. Les pourcentages sont relatifs aux parois dont les courbures épousent celles des contours d'écoulement de même pourcentage d'un jet s'étalant librement.

28. The comparison of the effect of the variously curved boundary walls are shown in Figure 11. Both sets of experiments referred to above are presented. As might be expected the walls curved to the lower percentage flow streamlines confine the jet somewhat, and so give a lower satisfactory U_0 and F_0 for a given x_s and h_s.

When comparing the straight walls with those curved to the 95 % streamlines the two observers covered a rather different range of phenomena in the pool. The observer covering the conservatively low speeds showed the straight wall line to lie at *higher* values of F_0, but converging with the curved wall line at about $F_0 = 10$: there are no higher velocities in this set of observations. The other observer, who regarded a jump as satisfactory when nearer the pool, showed the straight wall line to be at *lower* values of F_0, but it diverged from the curved wall line at about $F_0 = 6$: in this case the observations were carried up to the designed outlet F_0, and so the walls were tested at the speeds for which they were designed. It therefore appears that at the higher outlet speeds, near those for which the pool walls are designed, the curved walled pool shows a distinct advantage over the straight walls in that a lower sill or shorter pool is allowable. At lower speeds, below the F_0 at which the lines cross, the straight wall might have some advantage, but then the occasional high flood might jump the sill and cause high speeds in the downstream river. Since the curved walls would, in a prototype, economise in excavation and concrete, it is probably worthwhile to consider them in any specific design. Further model tests would still be necessary so that the engineer concerned can make his own decision as to the suitability of the position of the jump. The initial choice of pool length could be made from the curves of Figure 11, when other site conditions such as the height of the tunnel invert above the river level can be taken into consideration.

29. *Scaling.* In flows wherein there is little surface friction effect, as in this case, inertia and gravity forces dominate in the preservation and change of the movement and of the state of motion so that the dynamic similarity is realised according to the Froude law.

All quantities, therefore, of these model tests will be translated to any required prototype design according to the scale of Froude's law. Most of the graphs have been presented to assist in doing this. For a geometrically similar design of size s times that of the model, the prototype velocity of flow is $s^{\frac{1}{2}}$ times that of the model and the prototype discharge is $s^{5/2}$ times that of the model.

30. For instance, if we take a prototype spillway tunnel of 14 ft diameter (which is fairly common all over the world), the prototype-model scale related to a 4 inch diameter pipe model is 42 to 1. Thus a velocity of 1 ft/sec in the model represents a prototype velocity of 6.48 ft/sec, and 1 cusec model discharge is equivalent to 11,400 cusecs in the prototype. Extending the test results for $F_0 = 15.5$ ($U_0 = 12.9$ ft/sec and $Q = 1.13$ cusec) in the model

to a prototype (linear scale of 42.1) will, therefore, give an outlet velocity of 83.5 ft/sec and discharge of 12,900 cusecs in the prototype.

31. To sum up: the bulk of the flow (and of the energy) of a spreading jet of water from a tunnel (up to 80 % of the total flow) was found to be contained in approximately the middle third of its width; as a result it is not worthwhile with regard to energy dissipation to provide much more basin width outside the middle third zone than is necessary to reduce excessive waves reflected from the side. A properly placed hump of the right geometry encourages quicker and more evenly distributed spreading and, therefore, gives better energy dissipation in a stilling basin. The cavity which forms behind the hump itself contributes to better spreading and slower movement of the stream downstream. Because of the likelihood of damage due to oscillatory formation and collapse of the cavity resulting from the retarding force of the end-sill a hump is not recommended for use in short stilling basins for high flows ($F_0 \gg 10$). In the absence of any such force, however, there does not appear to be any more danger due to the cavity than happens with any other forms of baffle in a stilling basin.

References

[1] Elevatorski (E.). — Hydraulic Energy Dissipators. *McGraw-Hill Book Co.*, New York.

[2] Ven te Chow. — Open Channel Hydraulics. *McGraw-Hill Book Co.*, New York.

[3] Muckel (D. C.). — Research in Water Spreading. *Proc. A.S.C.E.*, Vol. 77, Dec. 1951.

[4] Kusnetzow. — Die Fliess Bewegung bei plözlicher Verbreiterung des Strombettes. *Hydrotechnisches Bauwesen*, No. 6, 1958.

[5] Unny (T. E.). — The Spatial Hydraulic Jump. *9th Convention of the International Association for Hydraulic Research*, Dubrovnik, Yugoslavia. 1961, p. 32.

[6] Rouse (H.), Bhoota (B.) and Hsu (En-Yun). — Design of Channel Expansions. *Proc. A.S.C.E.*, Vol. 75, 1949, p. 1369.

Résumé

Les ouvrages de sortie des galeries de déversoir

par
J.M.K. Dake *
et
J.R.D. Francis **

L'article décrit des essais en laboratoire à petite échelle, avec un modèle comportant une conduite débitant de l'eau sur un plan horizontal et situé au niveau du plafond de la conduite. Ce jet d'eau s'étale, et l'on détermine les filets liquides de l'écoulement en explorant les champs des vitesses et des charges totales (voir la figure 3). La figure 4 montre la répartition de l'énergie totale dans les différentes sections transversales, et la figure 5 représente les profils supérieurs. On montre, à partir de ces mesures, que des bajoyers courbes, et dont le tracé est donné par l'équation :

$$z/d_0 = C\,(x/E_0)^{1,6} + 0,5$$

contiendront tout juste 85 % de l'écoulement si $C = 2$, et 95 % de l'écoulement si $C = 2,75$ (x étant la distance suivant l'axe de la conduite, z la distance horizontale à travers l'écoulement, et E_0, l'énergie cinétique relative de la conduite de sortie). Par ailleurs, le profil superficiel est donné, approximativement, par la relation :

$$y = \frac{A_1 d_0^2 K}{x} \exp\,(-\alpha z^2/x^2)$$

dans laquelle y est la hauteur verticale du plan d'eau, A_1 est une constante dont la valeur est fonction de la forme de la sortie, K et α sont des fonctions dépendant du nombre de Froude relatif à la sortie $U_0^2/gd_0 = F_0$. Des conduites présentant une section triangulaire, avec le sommet du triangle en bas, étalent l'écoulement sensiblement plus rapidement que des conduites de section circulaire, ou triangulaire avec le sommet en haut (voir la figure 6).

* M. Sc. Tech. On leave from Kwame Nkrumah University of Science and Technology, Kumasi, Ghana.

** Manchester College of Science and Technology.

Des essais ont également été effectués avec une pyramide de faible hauteur (une bosse) disposée symétriquement sur le plan aval, de manière à établir un gradient de pression latéral dans l'écoulement. On a pu constater que le jet s'étalait plus rapidement lorsque cette bosse était présente que lorsqu'elle était absente (voir la figure 8 *b*). L'efficacité de cette bosse est fonction de sa position et de ses caractéristiques géométriques. Les meilleurs résultats ont été obtenus avec une bosse de la forme n° 4 (voir le tableau 1), située à l'endroit indiqué par le nombre de Froude relatif à la sortie (tableau 2).

Enfin, on a étudié le comportement d'une combinaison de la bosse, et des bajoyers, disposés de manière à constituer ensemble un véritable bassin de dissipation se terminant par un déversoir à son extrémité aval. Un ressaut se manifestait dans ce bassin, et on a observé l'emplacement le plus rapproché du déversoir correspondant à un ressaut convenable. La figure 10 montre que l'emploi de la bosse n° 4 a pour effet d'augmenter de 15 % le nombre de Froude pour lequel le bassin de dissipation perd toute son efficacité. La figure 11 montre le fonctionnement comparatif de plusieurs bajoyers courbes différents. Les divers observateurs ont éprouvé des difficultés en ce qui concerne l'interprétation d'un ressaut convenable, de sorte qu'il serait nécessaire que toutes décisions concernant une étude particulière de ce genre soient prises par l'ingénieur ayant exécuté l'étude en question.